Performance Optimization of Double Absorption Heat Transformers Using Genetic Algorithm in Order to Minimize Physical Exergy Destruction

Sarang Ezazi[1*], Abdolreza Sadighmanesh[2]
[1]Department of Mechanic, Ahar Branch, Islamic Azad University, Ahar, Iran
[2]Department of Electrical Engineering, Ahar Branch, Islamic Azad University, Ahar, Iran
[1]Email: sarangezazi@gmail.com (Corresponding Author)
[2]Email: re.sadigh@gmail.com

ABSTRACT
In the present study, double absorption heat transformers that are known as a desirable technology for the reuse of medium level waste heat energy are investigated. The main parameter that is considered as well as others is physical exergy destruction. Through an optimization process by the Genetic algorithm, it is found that, the new configuration has 14.3% and 3.36% higher distilled water and the COP compared to those parameters for common third type DAHT. When it comes to the total exergy destruction, it is 5.7% higher in comparison to the third type DAHT. Thermodynamic analysis and optimization are performed through EES.
KEYWORDS: Absorption heat transformer, exergy destruction, energy, ECOP, desalination

1. Introduction

The optimum use of available existence energy resources in the world is an inevitable subject. In order to achieve this purpose, the importance of recycling or improving the quality of wasted thermal energy in industrial processes has always been the focus of experts in the field of energy research and development. One of the most desirable energy saving devices that operates with low or medium level temperature thermal energy is Absorption Heat Transformer (AHT). In other words, AHT is a device that transforms medium temperature dissipated heat energy to higher temperature heat energy through performing a series of processes [1]. Delivered high temperature heat energy is used then in other secondary processes such as Organic Rankine Cycle (ORC) power plants, carbon dioxide critical fluid cycle, and water purification systems, etc. Absorption Heat Transformers has a very low electrical energy consumption that results in reduced emissions of pollutants such as CO_2 [2]. Increasing energy costs do not affect heat transformer's operation and performance because, this technology does not require fossil fuel to run. Since the only rotary equipment of an AHT is pump, therefore its relatively simple structure, operation, and maintenance, along with long useful life, are among the other advantages of this system [3]. The International Energy Agency (IEA) has introduced this device as a future technology although its industrial applications currently are very limited [4]. Rivera et al., investigated the exergy loss of a model of the double absorption heat transformer (DAHT), which is called the

first type double absorption cycle [5]. The second type double absorption cycle, which is an improved model of the first type double absorption transformers and has the possibility of simpler control, was proposed by Zhao et al., [6]. Another structure of DAHT that Mostofizadeh et al., [7] had made experimentally and known as the third type DAHT was theoretically investigated by Zhao et al., [8] which was shown to have a higher COP than the first and second types. Hernandez et al., [9] introduced a new cycle for single absorption and double absorption systems based on the resorption of heat from the solution and refrigerant lines by heat recovery, which, although the working pressure is lower, but the COP is lower compared to the basic transformers. Qin et al., [10] investigated the ecological performance of single absorption systems by considering both COP and heat loss from the cycle. Wang et al., [11] investigated the effect of the temperature difference between the generator and evaporator on the performance of the dual absorption system proposed by Khamooshi et al., [12] and they stated that the best performance is obtained at the same temperature of generator and evaporator. Heredia et al. [13] reported an increase of about 20% in the COP of lithium bromide single absorption system by installing a heat pipe assembly instead of a condenser. Vakim et al. [14] performed the simulation of the single absorption model in order to eliminate the contradictions of the previous studies and obtained different results including the existence of an extremum point in the performance coefficient curve versus absorber temperature increase. Wang et al., [15] demonstrated a conventional, advanced exergy and exergoeconomic analyses simulation and showed that only 21.28% of the exergy destruction rates are avoidable by improvement. Mahmoudi et al., [16] performed a thermoeconomic analysis on a proposed cogeneration cycle and indicated a minimum total product unit cost of 42.6$/GJ, a maximum exergy efficiency of 27.9%, and a maximum distilled water mass flow rate of 0.53 kg/s. Tang et al., [17] investigated the system performance enhancement brought by an AHT on the supercritical CO_2 Brayton cycle and repoted a 4.96% higher exergy efficiency than that of the sCO_2 system.

In the present study, the third type DAHT is selected based on its wide range applications and its performance from energy and exergy destruction point of view is compared to a new configuration of double absorption heat transformer [18]. An optimization based on neural networks is performed to achieve more clarified behavior of cycles in order to minimize exergy destruction.

2. Description of Cycles

An impure water desalination system attached to third type DAHT that is introduced by Khamooshi et al., [12] is shown in fig. 1. In the mentioned system, the wasted heat energy from industrial processes, Q_{Gen}, feeds generator at a relatively low temperature, T_{Gen}, in order to vaporize a portion of water refrigerant from LiBr-H_2O solution. The refrigerant flows to condenser where a phase change to saturated liquid occurs. Then, the condensed refrigerant is divided into two flow lines. One portion is pumped to evaporator, where receives a quantity of the waste heat, Q_{Eva}, at an intermediate temperature, T_{Eva}, and becomes saturated vapor. The other portion flows to Abs/Eva

via a pump at a higher pressure to produce steam at a higher temperature, $T_{Abs\backslash Eva}$. The steam in absorber will be absorbed to strong solution coming from the generator at higher temperature, T_{Abs}. This is an exothermic process in which, desired thermal energy, Q_{Abs}, at higher temperature, T_{Abs}, is released. Also, the strong solution already recovered some heat through two heat exchangers towards the absorber. The output weak solution from the absorber flows to the absorber-evaporator for absorbing the saturated vapour that comes from the evaporator. The recent process, is exothermic and some heat is produced, $Q_{Abs\backslash Eva}$, through it too. Impure water from outside of DAHT receives the Q_{Abs} and becomes partially evaporated. Finally, desired pure fresh water vapour is extracted through a separator.

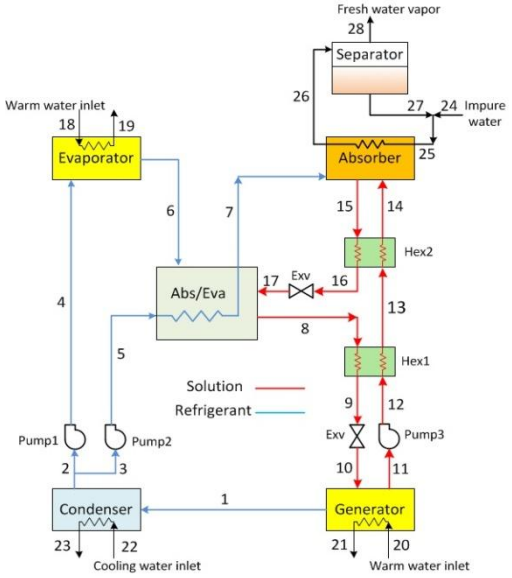

Fig.1.Schematic diagram of a DAHT coupled to a desalination system.

Fig. 2 shows the new configuration [18] in which strong solution leaving the generator and after passing through two heat exchangers is divided into two streams, one stream flows to the Abs/Eva and the other flows to absorber. The solution leaving the Abs/Eva is diluted only once and joins with the weak solution leaving the absorber, then flows to generator. It should be noted that the refrigerant path is the same in all cycles.

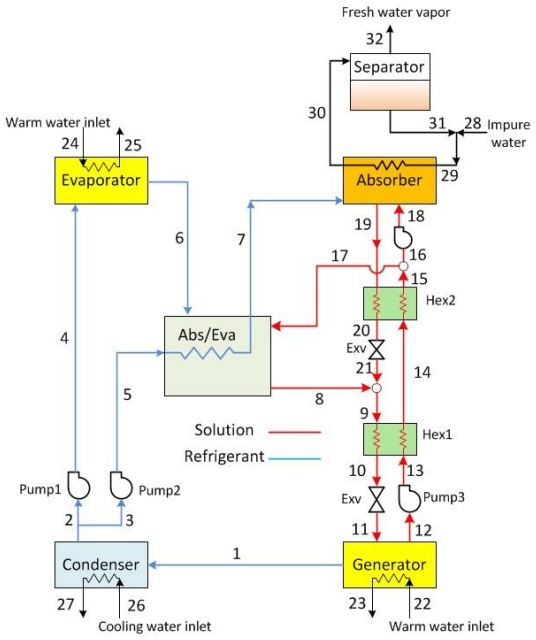

Fig. 2. Schematic diagram of new configuration of DAHT coupled to a desalination system.

3. MODELING

Basic assumptions and input parameters as well as essential equations necessary for analyses are mentioned in this section.

3.1. Assumptions

Some assumptions have been considered in order to model the cycles as follows:

(1) All processes are under steady conditions [2,3,7,12,15,16].
(2) Changes in kinetic and potential energies are neglected.
(3) Pressure drop because of friction in the piping system and components is ignored [2,3,4,6,7,16].
(4) Heat transfer to the environment is ignored for all components.
(5) Solution is saturated at the generator and the absorber outlet. Refrigerant is saturated at the evaporator and condenser outlet [2,3,4,5,6,7,12,].

(6) The input energy of the cycles is supplied from a heat source with temperature range of 90~100°C [3,12].
(7) The amount of input heat energy supplied to the evaporator is assumed to be the same in all cycles and temperatures of the generator and the evaporator are equal [3,12].

Also the range of values of modeling input parameters are expressed in Table 1.

Table 1. Input parameters

parameter	value
T_{con} (°C)	20~30
T_{eva}= T_{gen} (°C)	80~90
$T_{abs/eva}$ (°C)	105~115
T_{abs} (°C)	130~165
$T_{heat\ source}$ (°C)	T_{eva}+10
Max. mass rate of heat source (kg/s)	20
$T_{cooling\ water}$ (°C)	T_{con}-4
Mass flow rate of cooling water (kg/s)	13.8
η_{HEX} (%)	80

3.2. Performance evaluation

In order to evaluate the thermodynamic performance of the double absorption heat transformer cycles discussed in this research, it is first necessary to consider each of the mentioned cycle components as a control volume. Then the principles of conservation of mass according to equations 1 and 2, as well as the principle of conservation of energy i.e. equation 3, should be checked in each case.

$$\sum_i \dot{m}_i = \sum_e \dot{m}_e \quad (1)$$

$$\sum_i \dot{m}_i x_i = \sum_e \dot{m}_e x_e \quad (2)$$

$$\dot{Q}_{cv} + \sum_i \dot{m}_i h_i = \sum_e \dot{m}_e h_e + \dot{W}_{cv} \quad (3)$$

The coefficient of performance for the heat transformer cycle is defined as the ratio of the useful heat available at the output of the system to the driving heat input to the system [12,17]:

$$COP = \frac{\dot{Q}_{abs}}{\dot{Q}_{eva} + \dot{Q}_{gen}} \quad (4)$$

The exergy efficiency, which is needed to compare the performance quality of the cycles to each other, is defined as the subtraction of the exergy of the outgoing heat from the evaporator to the exergy of the incoming heat to the evaporator and generator [5]:

$$ECOP = \frac{\dot{Q}_{abs}(1-\frac{T_0}{T_{abs}})}{\dot{Q}_{eva}(1-\frac{T_0}{T_{eva}}) + \dot{Q}_{gen}(1-\frac{T_0}{T_{gen}})} \quad (5)$$

Another very important characteristic in evaluation of the cycles performance is exergy destruction that indicates the amount of loss in useful potential of energy that should be avoided and is defined as follows:

$$\dot{Ex}_D = T_o \dot{S}_G \quad (6)$$

A set of equations that are solved for the third type DAHT and the new configuration is mentioned in Table 2 and 3 respectively.

Table 2. Energy equations of fig.1.

Item	Energy equation
Con	$\dot{Q}_{con} = \dot{m}_2 h_2 + \dot{m}_3 h_3 - \dot{m}_1 h_1$ $= \dot{m}_{22}(h_{23} - h_{22})$
Eva	$\dot{Q}_{eva} = \dot{m}_4(h_6 - h_4)$ $= \dot{m}_{18}(h_{18} - h_{19})$
Gen	$\dot{Q}_{gen} = \dot{m}_1 h_1 + \dot{m}_{11} h_{11} \quad \dot{m}_8 h_{10}$ $= \dot{m}_{18}(h_{18} \quad h_{19})$
Abs/Eva	$\dot{Q}_{abs/eva} = \dot{m}_8 h_8 - \dot{m}_2 h_6 - \dot{m}_{15} h_{17}$ $= \dot{m}_3(h_7 - h_5)$
Abs	$\dot{Q}_{abs} = \dot{m}_{15} h_{15} + \dot{m}_3 h_7 - \dot{m}_{11} h_{14}$ $= \dot{m}_{25}(h_{26} - h_{25})$
Hex 1	$T_{13} = T_{12} + (T_8 - T_{12})\eta_{HEX1}$ $\dot{Q}_{HEX1} = \dot{m}_8(h_8 - h_9) = \dot{m}_{12}(h_{13} - h_{12})$
Hex 2	$T_{14} = T_{13} + (T_{15} - T_{13})\eta_{HEX2}$ $\dot{Q}_{HEX2} = \dot{m}_{15}(h_{15} - h_{16}) = \dot{m}_{13}(h_{14} - h_{13})$
Exv	$h_i = h_e$

As stated above, the exergy destruction should be calculated. Therefore, the related equations are as follows:

Table 3. Energy equations of fig.2.

Item	Energy equation
Con	$\dot{Q}_{con} = \dot{m}_2 h_2 + \dot{m}_3 h_3 - \dot{m}_1 h_1 = \dot{m}_{26}(h_{27} - h_{26})$
Eva	$\dot{Q}_{eva} = \dot{m}_4 (h_6 - h_4) = \dot{m}_{24}(h_{24} - h_{25})$
Gen	$\dot{Q}_{gen} = \dot{m}_1 h_1 + \dot{m}_{12} h_{12} - \dot{m}_{11} h_{11} = \dot{m}_{22}(h_{22} - h_{23})$
Abs/Eva	$\dot{Q}_{ab/ev} = \dot{m}_8 h_8 - \dot{m}_6 h_6 - \dot{m}_{17} h_{17} = \dot{m}_3 (h_7 - h_5)$
Abs	$\dot{Q}_{abs} = \dot{m}_{19} h_{19} - \dot{m}_{18} h_{18} - \dot{m}_3 h_7 = \dot{m}_{29}(h_{29} - h_{30})$
Hex 1	$T_{14} = T_{13} + (T_9 - T_{13})\eta_{HEX1}$ $\dot{Q}_{HEX1} = \dot{m}_9 (h_9 - h_{10}) = \dot{m}_{12}(h_{14} - h_{13})$
Hex 2	$T_{15} = T_{14} + (T_{19} - T_{14})\eta_{HEX2}$ $\dot{Q}_{HEX2} = \dot{m}_{19}(h_{19} - h_{20}) = \dot{m}_{12}(h_{15} - h_{14})$
Exv	$h_i = h_e$

Table 4. Exergy destruction equations of fig.1.

Item	Equation
Con	$\dot{E}x_D = T_o(\dot{m}_2 s_2 + \dot{m}_3 s_3 - \dot{m}_1 s_1 - \dot{m}_{22} s_{22} + \dot{m}_{23} s_{23})$
Eva	$E\dot{x}_D = T_o(\dot{m}_6 s_6 + \dot{m}_{19} s_{19} - \dot{m}_4 s_4 - \dot{m}_{18} s_{18})$
Gen	$E\dot{x}_D = T_o(\dot{m}_1 s_1 + \dot{m}_{11} s_{11} - \dot{m}_{10} s_{10} + \dot{m}_{21} s_{21} - \dot{m}_{20} s_{20})$
Abs/Eva	$E\dot{x}_D = T_o(\dot{m}_8 s_8 + \dot{m}_7 s_7 - \dot{m}_5 s_5 - \dot{m}_{17} s_{17} - \dot{m}_6 s_6)$
Abs	$E\dot{x}_D = T_o(\dot{m}_{15} s_{15} + \dot{m}_{26} s_{26} - \dot{m}_{25} s_{25} - \dot{m}_{14} s_{14} - \dot{m}_7 s_7)$
Hex 1	$E\dot{x}_D = T_o(\dot{m}_{13} s_{13} + \dot{m}_9 s_9 - \dot{m}_{12} s_{12} - \dot{m}_8 s_8)$
Hex 2	$E\dot{x}_D = T_o(\dot{m}_{13} s_{13} + \dot{m}_9 s_9 - \dot{m}_{12} s_{12} - \dot{m}_8 s_8)$
Exv1	$\dot{E}x_D = T_o(\dot{m}_{10} s_{10} - \dot{m}_9 s_9)$
Exv2	$\dot{E}x_D = T_o(\dot{m}_{17} s_{17} - \dot{m}_{16} s_{16})$

Subsequently the same relations are applied to figure 2 as table 5:

Table 5. Exergy destruction equations of fig.2.

Item	Equation
Con	$\dot{E}x_D = T_o(\dot{m}_2 s_2 + \dot{m}_3 s_3 - \dot{m}_1 s_1 - \dot{m}_{26} s_{26} + \dot{m}_{27} s_{27})$
Eva	$E\dot{x}_D = T_o(\dot{m}_6 s_6 + \dot{m}_{25} s_{25} - \dot{m}_4 s_4 - \dot{m}_{24} s_{24})$
Gen	$E\dot{x}_D = T_o(\dot{m}_1 s_1 + \dot{m}_{12} s_{12} - \dot{m}_{11} s_{11} + \dot{m}_{23} s_{23} - \dot{m}_{22} s_{22})$
Abs/Eva	$E\dot{x}_D = T_o(\dot{m}_8 s_8 + \dot{m}_7 s_7 - \dot{m}_5 s_5 - \dot{m}_{17} s_{17} - \dot{m}_6 s_6)$
Abs	$E\dot{x}_D = T_o(\dot{m}_{30} s_{30} + \dot{m}_{19} s_{19} - \dot{m}_{29} s_{29} - \dot{m}_{18} s_{18} - \dot{m}_7 s_7)$
Hex 1	$E\dot{x}_D = T_o(\dot{m}_{10} s_{10} + \dot{m}_{14} s_{14} - \dot{m}_{13} s_{13} - \dot{m}_9 s_9)$
Hex 2	$E\dot{x}_D = T_o(\dot{m}_{15} s_{15} + \dot{m}_{20} s_{20} - \dot{m}_{14} s_{14} - \dot{m}_{19} s_{19})$
Exv1	$\dot{E}x_D = T_o(\dot{m}_{11} s_{11} - \dot{m}_{10} s_{10})$
Exv2	$\dot{E}x_D = T_o(\dot{m}_{21} s_{21} - \dot{m}_{20} s_{20})$

3.2. Optimization

In order to minimize exergy destruction of discussed absorption heat transformers, the Genetic algorithm is applied. The dependent variable is exergy destruction, while temperature of two main components of cycles (T_{Con} and T_{Abs}) are selected as independent ones within the given range according to table 1.

Results

4.1. Validation of analysis

In order to validate the thermodynamic analysis, the results of the present study for a specific case have been compared with the reference results [12] and are shown in figure 3. According to figure 3 it can be concluded that there is a good agreement between the results of the present study and results of the Khanmooshi et al., [12].

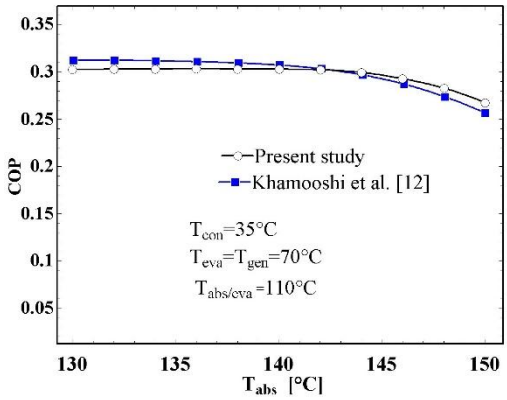

Fig. 3. Validation chart for thermodynamic analysis

4.2. Results of thermodynamic analysis

In this section, the effect of the working conditions of the cycle components on its performance has been examined. Figure 4 shows the effect of increasing the absorber temperature on the COP of the two structures discussed in this research. It is clear that the maximum value of the COP of the third type DAHT occurs in the temperature range between 150-165°C, while for the new configuration it is in the temperature range of 135-150°C. Basically, the reason for the faster reduction of the COP of the new configuration compared to the third type DAHT is the faster increase of the flow rate.

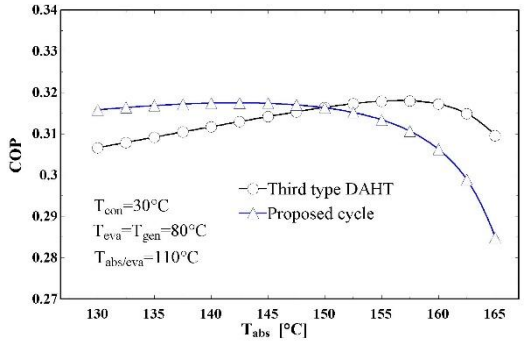

Fig. 4. The effect of the absorber temperature on the COP

According to figure 5, the maximum amount of purified water can be obtained by the new configuration. It should be noticed that although the COP of the existing third type DAHT in the temperature range after 150°C is higher than the new configuration but more produced heat energy is the main cause of more distilled water production by new configuration.

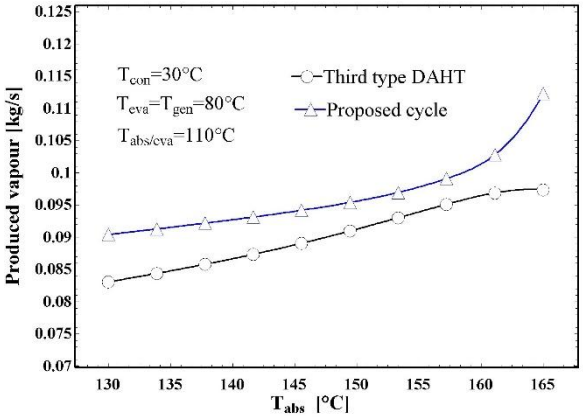

Fig. 5. The effect of absorber temperature on produced vapour

In the figure 6, the effect of absorber temperature increase on ECOP is illustrated. It is observed that the exergy coefficient of performance will tend the same as the energy coefficient of performance.

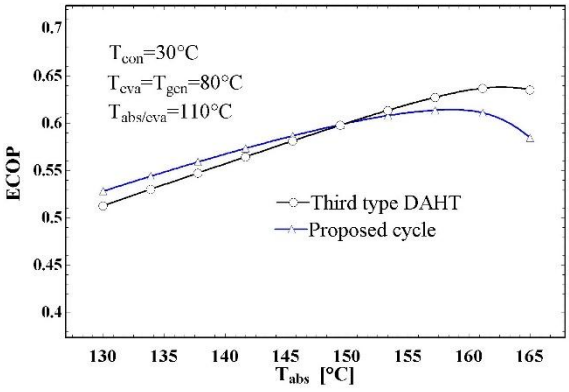

Fig. 6. The effect of the absorber temperature on distilled water production

Properties of state points of third type DAHT is stated in the table 6.

Table 6. Properties of state points of third type DAHT

state	ṁ (kg/s)	T (°C)	P (kPa)	x (%)	h(kJ/kg)	s(kJ/kg.K)
1	0.2008	80	4.246		2650	8.74
2	0.1009	30	4.246		125.7	0.4365
3	0.09986	30	4.246		125.7	0.4365
4	0.1009	30	47.37		125.7	0.4365
5	0.09986	30	143.2		125.8	0.4365
6	0.1009	80	47.37		2643	7.611
7	0.09986	110	143.2		2691	7.239
8	0.7325	110	47.37	45.69	246.2	0.7955
9	0.7325	96.35	47.37	45.69	213.7	0.7095
10	0.7325	50.31	4.246	45.69	213.7	0.7506
11	0.5317	80	4.246	62.94	210.2	0.4346
12	0.5317	80	143.2	62.94	210.2	0.4346
13	0.5317	104	143.2	62.94	255	0.5574
14	0.5317	140.8	143.2	62.94	325.3	0.7349
15	0.6316	150	143.2	52.99	327.9	0.9103
16	0.6316	123.4	143.2	52.99	268.7	0.7666
17	0.6316	116.6	47.37	52.99	268.7	0.7706
18	7.56	90		0	376.9	1.193
19	7.56	82		0	343.3	1.099
20	7.56	90		0	376.9	1.193
21	7.56	74.65		0	312.5	1.011
22	13.8	26		0	108.9	0.381
23	13.8	34.78		0	145.7	0.502
24	0.09126	25		0	104.8	
25	15	99.55		0	417.2	1.302
26	15	100	101.3	0.6084	432.8	1.344
27	14.91	100	101.3	0	419.1	1.307
28	0.09126	100	101.3	100	2676	7.354

Total exergy destruction ($Ex_{D,total}$) of discussed cycles that is defined as summation of exergy destruction of all main components is illustrated through figures 7 to 9. Figure 7, shows the comparison of the total exergy destruction of both cycles versus absorber temperature increase. In figure 8, the variation of total exergy destruction of both transformers is being seen as a function of condenser temperature variation. Finally, the dependency of total exergy destructon to evaporator and generator temperature is expressed in figure 9. As it is observed, The overall effect of increasing the temperature of the absorber on total exergy destruction is incremental in third type DAHT. This is because of mixing of refrigerant and strong solution in the absorber that results more vapour production. Total exergy destruction has a slightly decrease in lower absorber temperatures in the new configuration, because the strong solution flow to the absorber in comparison with the refrigerant flow is less, but this process changes as absorber temperature increases to values more than 150^{o}C.

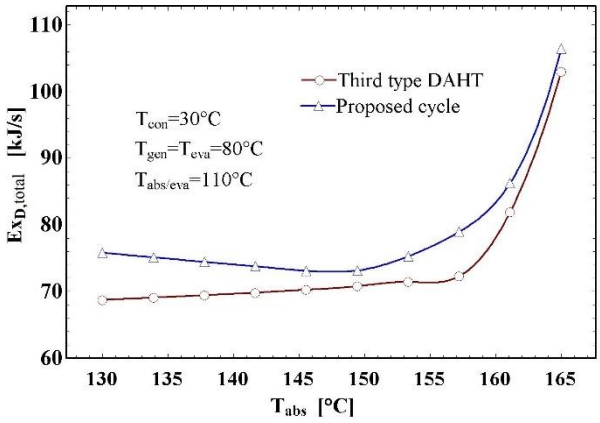

Fig. 7. The effect of absorber temperature on total exergy destruction of cycles

It is observed from figure 8 that as condenser temperature increases, heat losses in the cycles decrease and less heat will dissipate to the environment. Therefore total exergy destruction tends to decrease in both transformers.

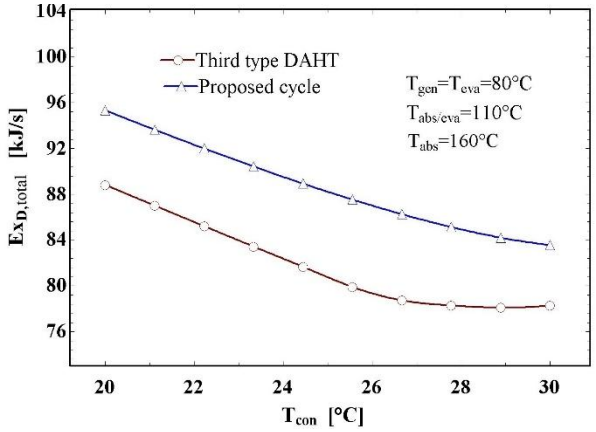

Fig. 8. The effect of condenser temperature on total exergy destruction of cycles

Figure 9, reveals that any increase in temperature of the evaporator will increase total exergy destruction, because more refrigerant will produce in both cycles, in other words, more phase change from liquid to vapour occurs in the evaporator.

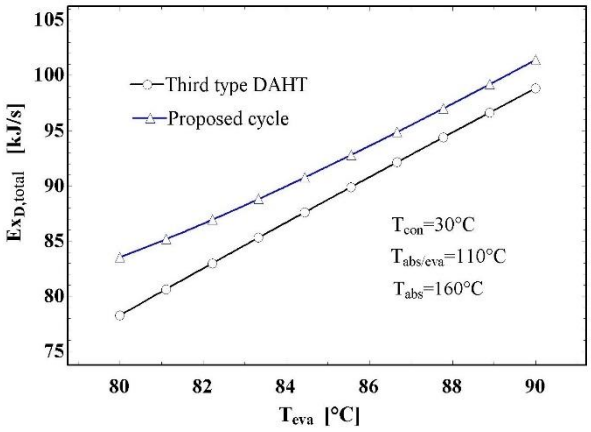

Fig. 9. The effect of evaporator temperature on total exergy destruction of cycles

4.3. Results of optimization

In order to achieve minimized total exergy destruction in both transformer cycles, an optimization has been performed through Genetic algorithm. The results of optimization are shown in table 7.

Table 7. Optimization results

	T_{Abs} (°C)	T_{Con} (°C)	$\dot{m}_{vap}$ (kg/s)	COP	$Ex_{D,total}$ (kJ/s)
3rd type DAHT	130	30	0.08307	0.3066	68.73
New configuration	148.1	30	0.09495	0.3169	72.65

As the results show, the new configuration demonstrated better results from produced vapour amount and COP point of view, but when it comes to total exergy destruction, the third type DAHT treats better.

5. CONCLUSIONS

In the present study, thermodynamic analysis and optimization of a new configuration of double absorption heat transformer integrated with a water desalination system are performed. The purpose of this article was to compare the new configuration of double absorption heat transformer with common third type DAHT from the exergy destruction point of view and to find specific operation conditions in order to minimize the total exergy destruction of both cycles. Analysis and optimization process has been performed through EES software [19]. The results showed that distilled water amount and the COP of new configuration are 14.3% and 3.36% higher than those parameters for common third type DAHT respectively. When it comes to the total exergy destruction, it is 5.7% higher in comparison to the third type DAHT.

Refrences

[1] Parham K., Khamooshi M., Tematio D.B.K., Yari M., Atikol U., "Absorption heat transformers– a comprehensive review," *Renewable and Sustainable Energy Reviews*, vol. 34, pp. 430-452, 2014.

[2] Zhao Z., Zhou F., Zhang X., Li S., "The thermodynamic performance of a new solution cycle in double absorption heat transformer using water/lithium bromide as the working fluids," *International Journal of Refrigeration*, vol. 3, no. 26, pp. 315-320, 2003.

[3] Horuz I., Kurt B., "Absorption heat transformers and an industrial application," *Renewable Energy*, vol. 10, no. 35**,** pp. 2175-2181, 2010.

[4] Donnellan P., Cronin K., Byrne E., "Recycling waste heat energy using vapour absorption heat transformers: a review," *Renewable and Sustainable Energy Reviews*, vol. 42, pp. 1290-1304, 2015.

[5] Rivera W., Best R., Hernández J., Heard C. L., and Holland F. A., "Thermodynamic study of advanced absorption heat transformers-II. Double absorption configurations," *Heat Recovery Systems and CHP*, vol. 14, pp. 185-193, 1994.

[6] Zhao Z., Zhou F., Zhang X., and Li S., "The thermodynamic performance of a new solution cycle in double absorption heat transformer using water/lithium bromide as the working fluids," *International Journal of Refrigeration*, vol. 26, pp. 315-320, 2003.

[7] Mostofizadeh C. and Kulick C., "Use of a new type of heat transformer in process industry," *Applied Thermal Engineering*, vol. 18, pp. 857-874, 1998.

[8] Zhao Z., Ma Y., and Chen J., "Thermodynamic performance of a new type of double absorption heat transformer," *Applied Thermal Engineering*, vol. 23, pp. 2407-2414, 2003.

[9] Hernández-Magallanes J. A., Rivera W., and Coronas A., "Comparison of single and double stage absorption and resorption heat transformers operating with the ammonia-lithium nitrate mixture," *Applied Thermal Engineering*, vol. 125, pp. 53-68, 2017.

[10] Qin X., Chen L., and Xia S., "Ecological performance of four-temperature-level absorption heat transformer with heat resistance, heat leakage and internal irreversibility." *International Journal of Heat and Mass Transfer*, vol. 114, pp. 252-257, 2017.

[11] Wang H., Li H., Bu X., and Wang L., "Effects of the generator and evaporator temperature differences on a double absorption heat transformer-Different control strategies on utilizing heat sources," *Energy Conversion and Management*, vol. 138, pp. 12-21, 2017.

[12] M. Khamooshi, K. Parham, I. Roozbeh, and H. Ensafisoroor, "Applications of innovative configurations of double absorption heat transformers in water purification technology," *Desalination and Water Treatment*, vol. 57, pp. 8204-8216, 2016.

[13] M. I. Heredia, J. Siqueiros, J. A. Hernández, D. Juárez-Romero, A. Huicochea, and J. G. González-Rodríguez, "Energy saving into an absorption heat transformer by using heat pipes between evaporator and condenser," *Applied Thermal Engineering*, vol. 128, pp. 737-746, 2018.

[14] M. Wakim and R. Rivera-Tinoco, "Absorption heat transformers: Sensitivity study to answer existing discrepancies," *Renewable Energy*, vol. 130, pp. 881-890, 2019.

[15] Y. Wang, Y. Liu, X. Liu, Z. Wanxiang, P. Cui, Y. Mengxiao, L. Zhiqiang, Y. Sheng, "Advanced exergy and exergoeconomic analyses of a cascade absorption heat transformer for the recovery of low grade waste heat," *Energy Conversion and Management*, vol. 205, pp. 112392, 2020.

[16] S. M. S. Mahmoudi, A. D. Akbari, M. A. Rosen, "A novel combination of absorption heat transformer and refrigeration for cogenerating cooling and distilled water: Thermoeconomic optimization," *Renewable Energy*, vol. 194, pp. 978-996, 2022.

[17] J. Tang, Q. Zhang, Z. Zhang, Q. Li, C. Wu, X. Wang, "Development and performance assessment of a novel combined power system integrating a supercritical carbon dioxide Brayton cycle with an absorption heat transformer," *Energy Conversion and Management*, vol. 251, pp. 114992, 2022.

[18] S. Ezazi, Sh. Khalilarya, S. Jafarmadar, "Thermodynamic Analysis and Comparative Assessment of Proposed Schemes of Double Absorption Heat Transformer in Water Vaporization Process for Desalination," Journal of Mechanical Engineering, vol. 50, no. 4, pp. 11-20, 2021.
(Doi: 10.22034/jmeut.2021.9144)

[19] S.A. Klein, Engineering Equation Solver, version 9.43, F-Chart Software, 2013.